# The moderately-large-embedded-cluster method for metal surfaces; a density-functional study of atomic adsorption



1994 J. Phys.: Condens. Matter 6 8149

(http://iopscience.iop.org/0953-8984/6/40/007)

J. Phys.: Condens. Matter 6 (1994) 8149–8166. Printed in the UK

# The moderately-large-embedded-cluster method for metal surfaces; a density-functional study of atomic adsorption

S Krüger and N Rösch

Lehrstuhl für Theoretische Chemie, Technische Universität München, D-85747 Garching, Germany

Received 24 April 1994, in final form 24 July 1994

**Abstract.** A comparative study of atomic chemisorption at a metal surface is performed using free- and embedded-cluster models. A newly developed implementation of the moderately-large-embedded-cluster (MLEC) approach is employed to describe the coupling of a surface cluster to its crystalline environment modelled by a slab. All calculations are done in the framework of density-functional theory using the local-density approximation. The cluster calculations are performed with the accurate all-electron linear-combination-of-Gaussian-type-orbitals formalism. The electronic structure of the substrate slab model is described using a linear-combination-of-Slater-type-orbitals method. A modification of the original MLEC formalism allows its application to metal substrates. The method is used here for the first time in combination with a 'first-principles' calculational scheme for the optimization of adsorption geometries employing an extended multilayered substrate. For the examples of H and O adsorption on the Li(001) surface clusters of different sizes are examined to explore the effects of embedding and the range of applicability of the MLEC method. The most pronounced effects observed are related to the charge rearrangement induced by adsorption. It is demonstrated that embedded clusters mirror the surface polarization of the Li(001) substrate and that the unphysical polarizability of free-cluster models is quenched due to embedding.

## 1. Introduction

The cluster-model approach has proven very useful for theoretical investigations of the adsorption of isolated atoms and molecules at solid surfaces [1–5]. The representation of an adsorption site by a finite number of substrate atoms rests on the assumption that the adsorbate–substrate interaction may be considered to exert only a locally confined perturbation on the substrate. A major attraction of this conceptually simple strategy for tackling an inherently complicated problem is connected to the fact that it makes a wealth of methods and interpretative tools of quantum chemistry available for the treatment of chemisorption. On the other hand, the successful application of this type of model requires a careful consideration of its deficiencies, such as the artificial boundary conditions and the discrete substrate density of states.

A variety of improvements have been suggested to overcome the difficulties of the cluster approach. Most of them are based on heuristic or physically motivated modifications of the cluster boundary conditions [6–10]; only a few exploit the complete substrate electronic structure by means of accurate Green-function methods [11–16] or other approaches [17, 18] aiming at a proper cluster embedding. The moderately-large-embedded-cluster (MLEC) method [19, 20] and its improvements [21, 22] use a Green-matrix formalism to couple a locally perturbed cluster to its crystalline environment. The representation of the electronic structure of the whole system by local orbitals provides the basis for the introduction

0953-8984/94/408149+18$19.50  

of approximations in the spirit of the cluster model. A computational procedure results in which the computational effort is focused on the chemisorption cluster, because the tedious integrations normally burdening the application of Green-function methods have to be carried out only once.

The MLEC method is suited to treat the general class of problems characterized as local perturbations of periodic systems. Most of the work done so far with this approach is concerned with perturbations of covalent and ionic crystals or surfaces [19, 20, 22–24]. Only one test calculation, employing an s-band tight-binding model, explored the applicability to a metal substrate [25]. Previously two approximate implementations of the method, employing large clusters to represent the cluster environment, were used to examine H [26] and $H_2$ [27] adsorption on Li(001). For H adsorption the on-top site was considered and only results of a Mulliken population analysis were discussed. The study on $H_2$/Li(001) examined the adsorption energetics along a fixed reaction path by embedding an $Li_4$ cluster in $Li_{10}$ and $Li_{14}$ substrate models representing the bridge site. Unfortunately no geometry optimization was carried out in either study, severely limiting an evaluation of the method by comparison with results from other theoretical approaches.

In the present work we describe our implementation of the MLEC formalism [19, 20] for metal substrates and we apply the MLEC method for the first time to adsorption at a voluminous metal substrate. Our approach is based on density-functional theory in the local-density approximation (LDA) [28]. While the embedded-cluster calculations are performed using the accurate all-electron linear-combination-of Gaussian-type-orbitals (LCGTO) method [5], an approximate Slater-type-orbital (STO) LDA code [29, 30] is used to determine the electronic structure of a metal slab modelling the substrate halfspace. It was necessary to modify the procedure of electronic density calculation in order to extend the applicability of the MLEC method to metallic systems. Furthermore, the SCF procedure was stabilized by self-consistently determining the cluster Fermi energy, thus avoiding instabilities that have plagued other implementations [20, 26, 27].

We present results for the atomic adsorption of H and O on an Li(001) surface, modelling the substrate by a five-layer slab. This work extends our preliminary study [31], which employed a monolayer-substrate model. A series of free and embedded clusters of different size is examined to validate our implementation and to characterize and rationalize the effects of embedding. H adsorption at the on-top and fourfold sites is treated, probing the adsorption properties of the 'naked'- and embedded-cluster models at different absorbate–substrate distances. To further clarify the cluster size required to meet the fundamental assumptions underlying the MLEC approach, O adsorption at a fourfold site of Li(001) is studied as a case of strong perturbation.

In the first part of this paper we summarize the MLEC formalism to provide a basis for the discussion of the salient features of the present implementation. In the second part we describe the cluster models in detail and discuss the effects of embedding on unperturbed surface clusters. Then we present results for atomic adsorption on Li(001), focusing on the consequences of embedding and on cluster size effects.

## 2. Method

### *2.1. General theory*

The MLEC formalism has been discussed several times in the literature [19, 20, 26, 27], but a brief review will facilitate the presentation of those points that are particular to the present

implementation and that are a prerequisite for the extension of the MLEC formalism to metallic substrates.

The absorption of a single atom or molecule on a crystal surface may be taken as a local perturbation of an otherwise perfectly ordered system. A Green-function formalism is well suited to solve the corresponding electronic structure problem provided the complete electronic structure of the unperturbed substrate surface is accessible. The Green operator **G** is defined as

$$\mathbf{QG} := ((e + \mathrm{i}\eta) - \mathbf{H})\mathbf{G} = 1. \tag{1}$$

**H** denotes an arbitrary effective one-electron Hamilton operator and **Q** is introduced as a shorthand for the inverse Green operator. The essential task of an embedded-cluster calculation is the determination of the Green function of the whole system in terms of the Green function of the unperturbed substrate and the perturbing potential generated by the absorption. To set the stage for the introduction of approximations, the system under consideration is divided in three parts: the adsorbate denoted by A, a finite region B around the adsorption site that is affected by the adsorbate–surface interaction and the unperturbed remainder D of the substrate halfspace. Part A and B together form the so-called 'chemisorption cluster' C. Assuming a basis set of functions localized at the atomic sites, this paritioning formally translates into a corresponding blocked matrix representation of all relevant operators.

Two important approximations are adopted in the MLEC approach [19, 20]. First, the local nature of the perturbation is exploited by assuming the perturbative potential to be confined to the chemisorption cluster C. A second approximation is employed to simplify the coupling of the cluster to the indented solid D. The cluster B is assumed to be chosen large enough so that it not only comprises all effects of adsorption, but also features an unperturbed boundary region towards the substrate. It seems physically plausible that this assumption may be satisfied for a 'moderately large' cluster. Exploiting these approximations the principal equation of the MLEC approach may be derived [20]:

$$\mathbf{G}_{CC} = (\mathbf{Q}_{CC})^{-1}\mathbf{J}_{CC} =: \bar{\mathbf{G}}_{CC}\mathbf{J}_{CC}. \tag{2}$$

The local Green matrix is obtained by correcting the Green matrix of an isolated cluster $\bar{\mathbf{G}}_{CC}$ using the matrix

$$\mathbf{J}_{CC} := \mathbf{Q}^{f}_{CC}\mathbf{G}^{f}_{CC} \tag{3}$$

which describes the coupling to the unperturbed surrounding [20].

The following SCF procedure results:

$$\mathbf{H}_{CC}\bar{\mathbf{A}} = \mathbf{S}_{CC}\bar{\mathbf{A}}\mathbf{E} \tag{4a}$$

$$\mathbf{P}_{CC} = -\frac{1}{\pi}\,\mathrm{Im}\int_{-\infty}^{+\infty}\mathbf{G}_{CC}(e)\Theta(E_F - e)\,\mathrm{d}e \tag{4b}$$

$$\mathbf{H}_{CC} = \bar{\mathbf{H}}_{CC}(\mathbf{P}_{CC}) + \Delta\mathbf{H}^{f}_{CC}. \tag{4c}$$

In the first step an eigenvalue problem has to be solved for the isolated cluster C employing the corresponding submatrix of the Hamiltonian of the entire system. The one-electron orbitals $\bar{\mathbf{A}} = (\bar{a}_{\mu i})$ and energies $\mathbf{E} = (e_i)$ of this intermediate subsystem are used to construct

$\bar{\mathbf{G}}_{CC}$. Inclusion of the coupling to the substrate results only in a matrix multiplication (2) where the coupling matrix $\mathbf{J}$ is independent of the absorbate. Thus, no costly update is required during the SCF procedure. After integration, one obtains the density matrix $\mathbf{P}_{CC}$ of the perturbed cluster density and proceeds to construct the effective cluster Hamiltonian $\bar{\mathbf{H}}$ and adds the contributions $\Delta\mathbf{H}$ from the nuclei and the electronic potential of the indented solid. This correction term cannot be calculated directly because in density-functional theory the density enters the effective Hamiltonian in a non-linear fashion. Nevertheless, exploiting the MLEC approximation, which assumes this correction to be independent of the absorbate, one has

$$\Delta H^{f}_{CC} = ((H^{f}(P^{f}))_{BB} - \bar{H}_{BB}(P_{BB}))_{C}. \tag{5}$$

$\bar{\mathbf{H}}_{BB}$ denotes the effective Hamiltonian matrix of the unperturbed but embedded cluster B and depends on the density matrix $\mathbf{P}_{BB}$, which is obtained in analogy to (4*b*). For a given cluster, $\Delta\mathbf{H}$ has to be determined only once in the subspace B, but before employing it in a perturbed-cluster calculation it has to be projected on the absorbate-dependent basis of the chemisorption cluster as indicated by the subscript C.

To derive working equations one proceeds by expressing the substrate Green matrix occurring in $\mathbf{J}$ in terms of the projected density of states $\rho$

$$G^{f}_{\mu\nu}(e) = \mathcal{P}\int_{-\infty}^{+\infty} \frac{\rho^{f}_{\mu\nu}(t)}{e-t}\,dt - i\pi\rho^{f}_{\mu\nu}(e) \tag{6}$$

and inserts this relation and its discrete counterpart for the cluster Green matrix $\bar{\mathbf{G}}$ into (4*b*). Finally, one arrives at a more handy form for the density matrix [20]:

$$\begin{aligned} P_{\mu\nu} &= 2\sum_{i} \bar{a}_{\mu i}\bar{a}_{\nu i}\Theta(E_F - e_i) \qquad \mu \in C, \nu \in A \\ P_{\mu\nu} &= 2\sum_{i,\alpha\in B} \bar{a}_{\mu i}\bar{a}_{\alpha i}M_{\alpha\nu}(e_i) \qquad \mu \in C, \nu \in B \end{aligned} \tag{7}$$

which may be interpreted as a one-particle density matrix where the occupation numbers are partially replaced by an energy-dependent coupling matrix

$$\begin{aligned} M_{\mu\nu}(e) = \mathcal{P}\int_{-\infty}^{+\infty} \frac{tS_{\mu\alpha} - H^{f}_{\mu\alpha}}{t-e}\rho^{f}_{\alpha\nu}(t)\Theta(E_F - t)\,dt \\ - \mathcal{P}\int_{-\infty}^{+\infty} \frac{eS_{\mu\alpha} - H^{f}_{\mu\alpha}}{t-e}\rho^{f}_{\alpha\nu}(t)\Theta(E_F - e)\,dt. \end{aligned} \tag{8}$$

This MLEC matrix only depends on the electronic structure of the unperturbed surface and thus all integrations can be performed prior to entering the SCF process. Thus, in comparison to other Green-function methods [11, 13–16], the MLEC approach leads to a very economic calculational procedure.

The coupling matrix $\mathbf{M}$ is known to be a very smooth function of the energy [19, 26, 27], except for a logarithmic pole at the Fermi level. This pole originates in the discontinuity of the step function representing the electronic distribution function in the definition of the density matrix. If there is a non-vanishing density of states at the Fermi level, the principal-value integration cannot be carried out for $e = E_F$. For insulating materials and for small

metallic clusters, the spectrum of one-electron energies, even in the LDA, features a large enough gap to prevent numerical complications. On the other hand, for metallic clusters of moderate size, as required by the MLEC method, a dense manifold of states around $E_F$ will obstruct convergency.

To extend the applicability of the MLEC approach to metallic systems and to remove the discontinuity we suggest 'broadening' the step function in a pragmatic fashion replacing $\Theta$ for $e \in [E_F - \delta, E_F + \delta]$ by

$$\Theta_b(E_F - e) = \tfrac{1}{2}(1 + \sin[\pi(E_F - e)/2\delta]). \tag{9}$$

Then the principal-value integration in (8) can always be performed. After straightforward, but somewhat tedious, calculations one obtains more complicated working equations. Smoothing the step function affects the MLEC matrix at all energies, but only near the Fermi level are considerable changes found. However, their ultimate consequences for physical observables are negligible in comparison to the general accuracy of the method since embedding in general broadens the Fermi edge through the non-integral effective occupation numbers of the cluster orbitals.

Summarizing the MLEC formalism, the following computational procedure results:

(i) self-consistent determination of the substrate electronic structure;

(ii) construction of the substrate projected density of states $\boldsymbol{\rho}^f$ and of the Hamilton matrix $\mathbf{H}^f$ in a localized basis;

(iii) choice of surface cluster B, gathering of the corresponding submatrices of $\boldsymbol{\rho}^f$ and $\mathbf{H}^f$, determination of the MLEC matrix and the corrective term to the Hamiltonian;

(iv) self-consistent treatment of the absorption problem.

### 2.2. *Implementation*

The formal derivation of the MLEC method is implicitly based on the usage of localized basis functions for the treatment of the extended substrate as well as for the chemisorption cluster. Furthermore, the electronic structure of the periodic and of the local subsystem have to be described at an identical theoretical level. If these prerequisites are met the density of an unperturbed embedded cluster will properly reflect the electronic density distribution of the substrate [19]. Thus, it is necessary to use the same basis set and to carefully adapt the computational parameters in the crystal and the cluster calculation. In practice this is a delicate task. On the one hand, the basis set has to be localized enough to avoid overcompleteness problems in the calculation of the periodic substrate [29]. On the other hand, the proper description of the adsorbate-substrate bond requires an enhanced flexibility of the basis set. However, any given basis set will be locally more complete in a crystalline than in a cluster application due to periodicity. Other intrinsic differences between local and periodic calculations are given by features such as $k$-point sets and lattice sum truncation parameters.

These problems are lessened by using a large cluster as a substrate model [26, 27]. This cluster-in-cluster approach may be advantageous if one intends to fix only the boundary conditions. However, it will be necessary to choose computationally prohibitively large clusters in order to shield a subcluster chosen in accord with the MLEC assumptions from the artificial cluster boundary effects. Moreover, cluster substrate models have to be chosen in accord with the local symmetry of the perturbation under consideration while periodic models provide the basis for the embedding of any cluster representing a finite section of the substrate.

To achieve realistic boundary conditions a periodic treatment of the substrate seems essential. As our interest focuses on the absorption complex we opted for an approximate substrate description [29,30] to concentrate the computational effort on the cluster part. Thus we are free to choose specifically adapted basis sets for both the periodic and the molecular calculation. Closer inspection of the various quantities entering the local SCF procedure suggests that this approach might be successful. The corrective term $\Delta\mathbf{H}$ to the Hamiltonian is assumed to provide a small contribution to the cluster Hamiltonian. The coupling matrix is known to be a smooth stuctureless function of the energy; details of the substrate electronic structure are 'averaged' out due to the integration involved. These observations and the rather strong approximations underlying the MLEC formalism suggest that a moderate additional approximation on the substrate side of the calculation should be acceptable.

In our implementation, the first step of an embedded-cluster study consists in the determination of the energy bands and of the Bloch eigenfunctions of a suitable substrate slab model. Then the crystal wave functions are expanded in a richer basis chosen for the treatment of the chemisorption cluster, and the basic quantities for the calculation of the MLEC matrix as well as of $\Delta\mathbf{H}$, the substrate Hamiltonian $H^{\mathrm{f}}_{\mu\nu,g}$ and the projected density of states (PDOS)

$$\rho^{\mathrm{f}}_{\mu\nu,g}(e) = \frac{1}{A}\int \mathrm{d}^2k \sum_n a^{*\mathrm{f}}_{\mu n}(k)a^{\mathrm{f}}_{\nu n}(k)\mathrm{e}^{-\mathrm{i}k\cdot g}\delta(e - e_n(k)) \tag{10}$$

are determined in a real-space representation. In equation (10) Greek indices refer to basis functions in the slab unit cell; $g$ denotes a two-dimensional lattice vector. After choosing a local cluster B and identifying it with a portion of the substrate crystal, the corresponding matrix elements of $\mathbf{H}^{\mathrm{f}}$ and $\rho^{\mathrm{f}}$ have to be determined.

The partitioning of the matrix representations of the operators according to the definition of the various subsystems depends on the detailed form of the basis set employed and thus renders the method basis set dependent. We found that the straightforward procedure of partitioning according to the atomic centres on which the basis functions are anchored has some rather undesirable consequences [26,27]. First of all, in the case of Li, the integration of the cluster submatrix of the PDOS up to the Fermi energy yields always less than 90% of the electronic charge of the corresponding neutral cluster. This introduces artifacts into the electronic structure of the unperturbed embedded cluster, demanding a large corrective term to the Hamiltonian to restore the proper substrate-like electronic distribution. Moreover, the numbers of elements of the coupling matrix become fairly large, $10^2$ or more [26,27], if one follows this simple procedure. This leads to severe numerical problems for an accurate determination of the density matrix.

To overcome these difficulties a transformation to hybridized orbitals has been proposed for covalent materials [24] and various orthogonalization schemes have been used successfully for metals [26,27]. We opted for symmetrically orthogonalizing the substrate Bloch basis (separately for each $k$ point) constructed from the non-orthogonal basis set chosen for the cluster calculation. The orthogonal Bloch waves are used to represent the substrate eigenfunctions as well as $\rho^{\mathrm{f}}$ and $\mathbf{H}^{\mathrm{f}}$. Orthogonalizing the Bloch basis of the substrate is equivalent to the orthogonalization of the underlying localized basis set of infinite dimension. The symmetrical orthogonalization yields the most localized set of orthogonal functions in a least-squares sense [32]; they are localized at the same centres as the non-orthogonal localized functions they are derived from. Thus the assignment of matrix elements of $\rho^{\mathrm{f}}$ and $\mathbf{H}^{\mathrm{f}}$, both represented in the orthogonal basis, to the cluster or its

surroundings remains the same as for the non-orthogonal basis. In this new representation the partitioning yields a balanced distribution of the electronic charge between the cluster and its environment. Only for subclusters of an Li monolayer may charge neutrality be checked and it is found to be conserved to a fraction of about $10^{-4}$ [31]. For clusters designed to model the on-top absorption site on Li(001) small deviations from charge neutrality occur due to the surface polarization. The charges of $Li_5$, $Li_{14}$ and $Li_{26}$, for example, as determined by integration of the cluster submatrix of the PDOS, are $-0.30$, $+0.55$ and $-0.28$ au, respectively. For all clusters studied, these charges are found to fluctuate in qualitative agreement with the corresponding sums of atomic populations of the substrate slab (see subsection 3.2). For $Li_5$, $Li_{14}$ and $Li_{26}$, the slab population analysis yields charges of $-0.38$, $+0.48$ and $-0.24$, respectively. Thus, the symmetrically orthogonalized basis guarantees a satisfactory partitioning of the electronic density for a metallic substrate.

The orthogonalized basis set is only used to extract the cluster submatrices of the relevant quantities from their substrate counterparts. The coupling matrix and the corrective term to the Hamiltonian (equation (5)) have to be determined in a basis set suited for the treatment of the chemisorption cluster. For this reason $\rho^f$ and $\mathbf{H}^f$ are backtransformed to the non-orthogonal basis. Additionally, to exploit the symmetry of the chemisorption cluster in the local calculations, a second transformation is carried out to a basis consisting of symmetry-adapted linear combinations of the original basis functions according the point group of the cluster. The construction of the MLEC matrix requires only straightforward integration. The determination of $\Delta\mathbf{H}$ as the difference of matrices related to different functional spaces proceeds according to equation (5).

The only remaining question concerns the choice of the cluster Fermi energy during the SCF procedure. It seems to be most natural to use the substrate value. This choice is appropriate for non-metallic host systems exhibiting a large band gap, but it causes serious problems in the case of metals. The Fermi energy determines the cluster charge, which therefore depends on details of the level spectrum of the chemisorption cluster; it may even vary with the adsorbate geometry due to shifts of orbital energies or may be affected by the adsorbed species. The fundamental MLEC assumptions exclude a charge exchange between the cluster and its surroundings. Therefore, a perturbation-dependent charge of the chemisorption cluster is not consistent with the approximations of the method. Moreover, a fixed Fermi energy leads to charge oscillations, destabilizing the SCF procedure [20, 23, 26, 27]. In previous implementations damping procedures or even renormalization were necessary to achieve a well behaved SCF convergence [20, 23, 26]. The alternative approach of fixing the cluster charge is adopted here; this requires the self-consistent determination of a local Fermi energy. Unfortunately, it is not possible to unequivocally assign a charge to an individual atom in a compound system. For metals the charge rearrangement due to surface polarization will be small (see subsection 3.2 for Li(001)). Thus the total charge of a cluster will also be small and the charge per atom will decrease when the numbers of 'layers' in a cluster increases. Therefore, we decided to treat the embedded clusters as neutral, avoiding the introduction of an additional and ill defined computational parameter. The Fermi energy has to be calculated using the density matrix. Unfortunately, the MLEC formalism does not ensure the density matrix to be symmetric and positive definite; these properties are guaranteed only in the limit of infinite cluster size [19, 20]. In most of our calculations the density matrix exhibited small negative eigenvalues connected with high-lying unoccupied cluster orbitals; on the other hand, core orbitals were found to the associated with occupation numbers slightly larger than two. As expected, these effects diminished with growing cluster size and for moderately large clusters, typically containing more than 10–15 substrate atoms, the deviations of the eigenvalues from their

theoretically acceptable range were less than 0.03. To assure physically meaningful results we forced the eigenvalues to lie within the interval [0, 2] and determined the cluster charge by summing them.

### *2.3. Computational details*

For the electronic-structure calculations we use density-functional theory in the LDA [28]. The exchange–correlation potential is chosen according to the parameterization of Vosko and co-workers [33]. The electronic structure of a five-layer Li slab, modelling the Li(001) surface, is computed using an approximate two-dimensional (2D) STO LDA code [29, 30]. It employs a minimal basis of atomic orbitals built by combining six STO-type functions per angular momentum. Only valence electron bands are treated explicitly; the wave functions are orthogonalized to the relaxed atomic core orbitals. Additionally, the muffin-tin approximation is adopted for the exchange–correlation potential. The crystalline wave functions are evaluated for 24 special points [34] of the irreducible part of the Brillouin zone. For the local cluster calculations, both free and embedded, we apply an accurate all-electron LCGTO LDA code [5], which admits the use of flexible GTO basis sets. GTO basis sets are also used to represent the charge density and the exchange–correlation potential. The orbital basis sets are contracted using coefficients from atomic LDA orbitals (9s, 4p) → [4s, 2p] for Li [35], (6s, 1p) → [3s, 1p] for H [36] and (9s, 4p, 1d) → [4s, 3p, 1d] for O [36].

The PDOS is determined for 200 energies located equidistantly in the valence region of the Li slab. The 1s-derived core bands, exhibiting a nearly vanishing dispersion, are treated separately. The MLEC matrix is calculated and stored for 670 energies. These energy points are chosen with spacing increasing quadratically with growing distance from the Fermi energy in order to properly represent the coupling matrix near the Fermi level where it features a stronger variation. In the SCF procedure a linear interpolation is used to determine the coupling matrix for the various cluster orbital energies. The broadening parameter $\delta$ is fixed at 0.125 eV. This value may seem rather large, but test calculations on an $Li_9$ cluster confirmed the expected negligible influence of the additional broadening.

The cluster Fermi energy is evaluated iteratively from the density matrix until the total number of electrons is obtained with an absolute accuracy of better than $10^{-6}$. This procedure, together with the broadening of the MLEC matrix, yields a very satisfactory convergence behaviour. We found that, on average, an embedded-cluster calculation required fewer SCF cycles than a free-cluster calculation. As a result, the additional computational effort of the embedding is almost compensated by savings due to a faster convergence.

## 3. Applications

### *3.1. Geometry*

The ideal Li(001) surface exhibits a 2D square lattice with a lattice constant $a = 3.49$ Å chosen according to the bulk BCC phase of Li [37]. A five-layer slab is used to model this surface and to represent the unperturbed substrate for embedding cluster models of various adsorption sites.

On-top and fourfold adsorption sites will be considered in the following. The cluster models are constructed by successive addition of neighbouring shells starting with the atoms that form the adsorption site. The clusters will be denoted by $Li_n(m_1, m_2, m_3, \ldots)$, where $n$ denotes the total number of atoms and $m_i$ the number of atoms in the $i$th crystal layer

parallel to the (001) surface, starting with the surface layer. Individual groups of symmetry-equivalent atoms will be labelled by roman numbers, indicating the crystal layer they belong to, and a running index, increasing with the distance from the central symmetry axis of the cluster (see figure 1).

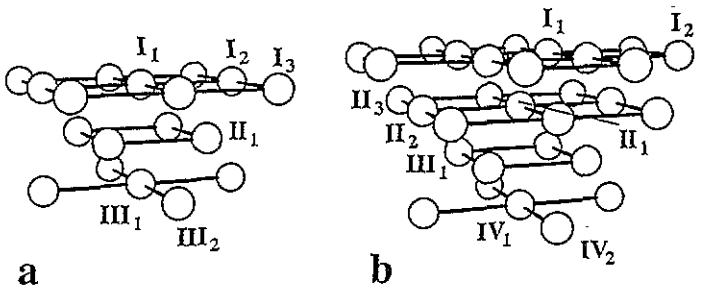


**Figure 1.** A sketch of the largest clusters investigated, (*a*) $Li_{18}$ for the on-top site and (*b*) $Li_{30}$ for the fourfold site. Groups of symmetry-equivalent atoms are labelled by roman numbers indicating the crystal layers (I = surface) and by a running index to distinguish the atoms within a layer.

In the case of on-top absorption only one substrate atom is in direct contact with the adsorbate. The cluster $Li_5(1, 4)$ includes the four nearest neighbours of this atom. Clusters comprising the second-nearest- and third-nearest-neighbour shells are $Li_{10}(5, 4, 1)$ and $Li_{18}(9, 4, 5)$, respectively. Additionally intermediate clusters, $Li_9(5, 4)$ and $Li_{14}(9, 4, 1)$, will be considered to elaborate on trends.

The fourfold adsorption site is more demanding with respect to embedding because more substrate atoms are in direct contact with the adsorbate. For small atomic adsorbates such as H, situated close to the surface, the four site atoms of the first layer will not be the nearest neighbours of the adsorbate. For adsorption heights smaller than $a/4 = 0.87$ Å, the central atom $II_1$ of the second layer will be closest to the adsorbate. Thus, for atomic adsorption at the fourfold site, five atoms have to be considered as being directly affected by the adsorption and one expects that a sufficient number of neighbours has to be provided for all of them to fulfill the MLEC assumptions. This will entail rather large clusters. $Li_{17}(4, 9, 4)$ comprises all first-nearest neighbours of the site atoms; $Li_{13}(4, 9)$ will also be studied to demonstrate the importance of the nearest neighbours of the second-layer site atom $II_1$. The cluster series is extended by $Li_{18}(4, 9, 4, 1)$, $Li_{26}(12, 9, 4, 1)$, completing the second-neighbour shell, and $Li_{30}(12, 9, 4, 5)$, including even some of the third-nearest neighbours of the site atoms.

### *3.2. Unperturbed surface clusters*

Already a comparison of results for free and embedded clusters will provide valuable insight into the consequences of embedding. Given the differences in the underlying calculational schemes discussed above, one should not expect quantitative correspondence of the results for an embedded cluster and a slab model. Nevertheless, significant signs of surface-like behaviour should be observable for embedded clusters.

MLEC embedding successfully removes the horizontal polarization at the border of free monolayer clusters, yielding a more homogeneous slab-like electron density [31]. Similarly, changes of the vertical polarization should be observable for the multilayer clusters under

consideration in the present study. A first, stringent test characterizing the electronic density distribution of embedded clusters is provided by core-level shifts [38]. The Li *1s*-derived levels of free clusters were found to be ordered according the coordination of the corresponding atoms. Embedding establishes a layerwise ordering of the core-level shifts, in good agreement with the shifts calculated from the slab core bands.

The cluster polarization may also easily be monitored by the normal component of its dipole moment. Free clusters were found to bear a small dipole moment whose sign and magnitude show no definite trend with increasing cluster size. This behaviour reflects the strong geometry dependence of the boundary polarization of the free clusters. For clusters embedded in the five-layer slab the dipole moment is always found to be positive (along the outside surface normal) and to grow monotonically with increasing cluster size. This may be rationalized by a positive surface charge of the slab that leads to a positive dipole moment for the surface unit cell. With increasing size the cluster extends over more unit cells and its dipole moment increases correspondingly. This explanation implies that the embedded cluster does not extend from one surface of the slab to the other.

The unusual finding of a positively charged metal surface is confirmed by Mulliken analysis of the five-layer Li slab. The rather compact basis set of the 2D STO LDA method [29] ensures that such an analysis provides at least qualitatively meaningful results. For the surface layer a small loss of electronic charge is observed, while the second layer exhibits a small negative charge. The Mulliken charges of the top three layers are 0.10, −0.12 and 0.06 au, starting with the surface layer. A qualitatively similar result is found from an accurate LCGTO LDA slab calculation using the FILMS code [39], where the same geometry and the same orbital basis set have been employed as in the present work. The charge of the individual layers was determined by layerwise integration of the electronic density, yielding values of 0.03, −0.03 and 0.00 au for the top three layers. In summary, the normal component of the dipole moment of embedded clusters reflects a polarization similar to that of the Li surface. The accumulation of electronic charge in the interior of the Li slab may be rationalized by the formation of 'three-centre bonds' similar to those known to stabilize small free Li clusters in their equilibrium geometry [40].

### *3.3. Hydrogen adsorption*

H adsorption has been studied as an example of a simple but chemically active local perturbation. On-top and fourfold adsorption sites have been considered, thus probing the properties of the cluster and embedded-cluster models of the Li(001) surface at different adsorbate–substrate distances.

The upper half of table 1 shows the results for on-top adsorption at free clusters. The adsorption bond distance stabilizes with increasing cluster size close to 1.7 Å; the frequency of the vertical stretching motion oscillates around 1040 $cm^{-1}$. The binding energy may be estimated to 1.5 eV. However, one should recall that this quantity is difficult to obtain from cluster-model studies [41]. These findings are similar to the results for H adsorption on large monolayer clusters [31] where an average bond distance of 1.66 Å and a frequency of 1100 $cm^{-1}$ have been calculated. The electron-density-related quantities, the Mulliken charge and the dynamical dipole moment $\partial\mu/\partial d$ indicate a negative charge on the adsorbate. As suggested by the differences between these results, the absolute values of the atomic charges obtained by both methods have to be taken with due caution, but for comparative purposes they are useful and indicative. The absorption-induced dipole moment is found to be always negative, in line with a negatively charged adsorbate. The relatively large fluctuations of this quantity may be rationalized by the cluster-dependent polarization of the 'surface', which is probed by the on-top absorption.

**Table 1.** H at the on-top site of Li(001): comparison of characteristic quantities of adsorption for free and embedded cluster models, Li–H bond distance $d$, frequency $\omega_0$ of the vertical stretching motion, binding energy $E_b$, adsorption-induced normal component of the dipole moment $\Delta\mu$, dynamical dipole moment $\partial\mu/\partial d$ and Mulliken charge $q$(H) of the adsorbate.

| Cluster | $d$ (Å) | $\omega_0$ ($cm^{-1}$) | $E_b$ (eV) | $\Delta\mu$ (debye) | $\partial\mu/\partial d$ (au) | $q$(H) (au) |
|---|---|---|---|---|---|---|
| Free | | | | | | |
| $Li_5$ | 1.66 | 1056 | 1.60 | −0.84 | −0.54 | −0.15 |
| $Li_9$ | 1.72 | 1016 | 2.16 | −0.14 | −0.50 | −0.15 |
| $Li_{10}$ | 1.70 | 1030 | 1.52 | −0.32 | −0.36 | −0.15 |
| $Li_{14}$ | 1.68 | 1064 | 1.79 | −0.90 | −0.29 | −0.12 |
| $Li_{18}$ | 1.69 | 1029 | 1.29 | −0.28 | −0.24 | −0.13 |
| Embedded | | | | | | |
| $Li_5$ | 1.84 | 1093 | 0.55 | −0.68 | −0.52 | 0.42 |
| $Li_9$ | 1.75 | 1197 | 0.30 | 0.00 | −0.07 | 0.32 |
| $Li_{10}$ | 1.71 | 1091 | 0.78 | −0.30 | −0.07 | 0.28 |
| $Li_{14}$ | 1.66 | 1041 | 0.86 | −0.22 | −0.04 | 0.23 |
| $Li_{18}$ | 1.66 | 1166 | 1.52 | −0.10 | −0.01 | 0.15 |

Some characteristics of the chemisorption cluster change due to embedding (see table 1). The bond distance shows a clear trend to slightly shorter values than in the case of free clusters. The bond distance is overestimated in small embedded-cluster models (relative to the values for the large clusters). This artifact occurs if the clusters are too small, thus violating the MLEC assumptions. As a consequence, the MLEC method and the implied boundary conditions bring about a substrate model that is too rigid, underestimating the polarizability of the substrate cluster. Along with the overestimation of the bond distance, the frequency of the vertical stretching motion and the binding energy are normally underestimated in small clusters [31]. These trends are not quite so obvious here, as the vibrational frequency fluctuates with cluster size more than in the case of free clusters. However, the binding energy has its smallest value for the smallest clusters. With the exception of $Li_{18}$, binding energies of embedded clusters are found to be smaller than for the corresponding free-cluster models. Leaving aside the two smallest clusters, which certainly do not fulfill the MLEC assumptions, one concludes that embedding reduces the electronic charge on the adsorbate compared to value of the free clusters. The dynamical dipole moment nearly vanishes; the Mulliken charges are even positive. For $Li_{14}$ and $Li_{18}$ the normal component of the induced dipole moment is found to be negative, but smaller than for the corresponding free clusters. The fact that the embedded-cluster model of H adsorption at the on-top site of the Li(001) surface attributes a more electronegative character to the adsorption site than the free-cluster model is in agreement with the positive surface polarization discussed above. This polarization of the substrate surface, observed for the five-layer slab, is a collective phenomenon, which is difficult to model by a finite cluster, but is represented by embedding.

Besides a more realistic modelling of the chemisorption interaction one would expect embedding to quench the fluctuations of calculated properties occurring for different cluster sizes. The results presented in table 1 clearly show that this expectation is not met. The increasing reliability of the approximations of the MLEC method with growing cluster size is one source of the cluster dependence of the results, especially for smaller clusters. Additionally, the unavoidable partitioning of the substrate function space that actually defines the cluster model affects the coupling matrix and the Hamiltonian. This dependence

of results on the choice of the local space treated self-consistently is also observed for less approximate embedding techniques [12, 22].

H adsorption at an on-top site probes the electronic structure of the Li surface at distances comparable to the (001) interlayer distance of 1.74 Å. At the fourfold site, on the other hand, the adsorbate comes into close contact to the top substrate surface layer. Various quantities determined for different cluster models, both free and embedded, are collected in table 2.

**Table 2.** H at the fourfold site of Li(001): a comparison of characteristic quantities of adsorption for free- and embedded-cluster models, adsorption height $h$ above the top layer of substrate atoms, frequency $\omega_c$ of the vertical stretching motion, binding energy $E_b$, adsorption-induced normal component of the dipole moment $\Delta\mu$ and Mulliken charge $q$(H) of the adsorbate.

| Cluster | $h$ (Å) | $\omega_c$ ($cm^{-1}$) | $E_b$ (eV) | $\Delta\mu$ (debye) | $q$(H) (au) |
|---|---|---|---|---|---|
| Free | | | | | |
| $Li_{13}$ | 0.20 | 652 | 2.54 | −0.12 | −0.21 |
| $Li_{17}$ | 0.09 | 899 | 2.43 | −0.01 | −0.18 |
| $Li_{18}$ | 0.07 | 903 | 2.41 | 0.09 | −0.20 |
| $Li_{26}$ | 0.14 | 793 | 2.47 | 0.23 | −0.21 |
| $Li_{30}$ | 0.16 | 791 | 2.78 | 0.31 | −0.24 |
| Embedded | | | | | |
| $Li_{13}$ | 0.93 | 1460 | 1.61 | −0.03 | 0.23 |
| $Li_{17}$ | 0.38 | 620 | 2.23 | −0.15 | 0.20 |
| $Li_{18}$ | 0.19 | 847 | 2.31 | 0.04 | 0.19 |
| $Li_{26}$ | 0.18 | 800 | 2.48 | 0.04 | −0.12 |
| $Li_{30}$ | 0.18 | 760 | 2.32 | 0.01 | −0.22 |

For larger clusters the adsorbate is situated about 0.2 Å above the top 'crystal' layer, corresponding to an Li–H bond distance of 1.95 Å for the nearest-neighbour substrate atom $II_1$ and of 2.48 Å for the top-layer site atoms $I_1$. The adsorption height is found to be smaller in free-cluster models, but the difference between the free cluster results and the apparently more stable results of embedded clusters decreases with growing cluster size. In both types of model, the frequencies of the vibrational motion are calculated at about 800 $cm^{-1}$. Unfortunately the corresponding potential well for H is very shallow, preventing an accurate numerical determination of vibrational excitations; thus harmonic frequencies are given here. For a cluster-model study, binding energies are found to be exceptionally stable as a function of cluster size. Again, the trend to lower binding energies due to embedding is apparent. The results for $Li_{13}$, strongly deviating from those of larger clusters, demonstrate the effects of a cluster choice that violates the MLEC assumptions. Here, the key is the number of nearest neighbours of the subsurface atom $II_1$ that lies closest to the adsorbate. Considerably better results are found for $Li_{17}$, a cluster that includes the four nearest neighbours of atom $II_1$ in the third crystal layer. Inspection of table 2 shows that the inclusion of suitable surroundings of the adsorption site is essential for embedded clusters, much more so than for the free-cluster models.

For adsorption at the fourfold site, the adsorbate charge can only be characterized by population analysis. The dynamical dipole moment is not suitable because the H is located close to the substrate surface. Taking into account larger clusters only, both free and embedded calculations yield a negative adsorbate charge. The values for the induced dipole moment seem to be at variance with this observation. They are positive for free clusters

and nearly vanishing, but also positive for their embedded counterparts. The more negative charge on the adsorbate in comparison with the on-top situation may be rationalized by the assumption that H interacts with the Li 'three-centre bonds' [40]. The resulting charge transfer occurs predominantly in the horizontal direction, parallel to the surface. Thus the counterintuitive values of the induced dipole moment have to be ascribed to a differing vertical polarization of free and embedded clusters and are not a direct consequence of adsorption. This picture of density redistribution due to adsorption is confirmed by difference density plots. Figure 2 shows the adsorption-induced changes in electronic density for the example of $Li_{30}$ along a diagonal cut through the surface unit cell. In the case of the free-cluster model, a loss of electronic charge is observed around the negatively charged adsorbate; this is most pronounced between the top and the subsurface layer of substrate atoms. Moreover the adsorption induces a counterpolarization extending even to the Li atom in the fourth subsurface layer. Cluster embedding confines these adsorption-induced effects essentially to the immediate surroundings of the adsorption site. The horizontal charge transfer to the adsorbate is more apparent here. The missing polarization of the 'lower' part of the cluster explains the smaller value of the normal component of the induced dipole moment. Moreover, the vanishing density change at the cluster border confirms that the cluster has been chosen large enough to satisfy the MLEC assumptions.

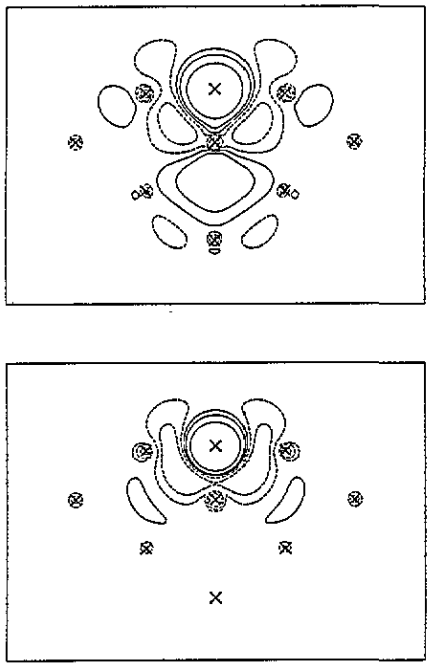

**Figure 2.** The adsorption-induced change of the electronic density $\Delta\rho = \rho(Li_{30}H) - \rho(Li_{30}) - \rho(H)$ for H adsorption at the fourfold site of Li(001): upper panel, free cluster; lower panel, embedded cluster. Contour lines are drawn for $\pm 0.00032$, $\pm 0.001$, $\pm 0.0032$ au; continuous and dashed lines correspond to positive and negative values, respectively. Crosses indicate the positions of the atoms.

In a Hartree–Fock configuration interaction study [42], using small double-layered free-cluster models, adsorption geometries and binding energies in qualitative agreement with

our results have been obtained. Unfortunately no analysis of the charge distribution has been undertaken. At variance with these and our results, a Hartree–Fock many-body perturbation-theory study [43] of H adsorption on Li(001) revealed longer bond distances by up to 0.15 Å for the on-top site; also, for both sites, binding energies fluctuate strongly with cluster size. These deviations from our results may be rationalized by the usage of 'optimized' lattice constants for each individual surface cluster, a strategy that seems questionable for substrate models with 10 atoms or fewer [43].

### *3.4. Oxygen adsorption*

O adsorption at the fourfold site provides an example for a strong electronegative perturbation of the Li(001) surface. In comparison to H adsorption stronger effects of embedding are to be expected. On the other hand, the problem of choosing a proper model with respect to embedding deserves more attention.

**Table 3.** O at the fourfold site of Li(001): a comparison of characteristic quantities of adsorption for free- and embedded-cluster models, adsorption height $h$ above the top layer of substrate atoms, frequency $\omega_0$ of the vertical stretching motion, binding energy $E_b$, adsorption-induced normal component of the dipole moment $\Delta\mu$ and Mulliken charge $q$(O) of the adsorbate.

| Cluster | $h$ (Å) | $\omega_0$ ($cm^{-1}$) | $E_b$ (eV) | $\Delta\mu$ (debye) | $q$(O) (au) |
|---|---|---|---|---|---|
| Free | | | | | |
| $Li_{17}$ | 0.02 | 403 | 7.61 | 0.09 | −0.75 |
| $Li_{18}$ | 0.01 | 403 | 7.70 | 0.14 | −0.76 |
| $Li_{26}$ | 0.00 | 413 | 7.64 | 0.01 | −0.76 |
| $Li_{30}$ | −0.01 | 413 | 7.31 | 0.01 | −0.77 |
| $Li_{38}$ | 0.01 | 389 | 7.26 | 0.05 | −0.79 |
| Embedded | | | | | |
| $Li_{17}$ | 0.15 | 328 | 6.00 | −0.34 | −0.96 |
| $Li_{18}$ | 0.21 | 299 | 6.05 | −0.30 | −1.00 |
| $Li_{26}$ | 0.05 | 379 | 6.31 | −0.06 | −0.88 |
| $Li_{30}$ | 0.01 | 398 | 6.17 | −0.06 | −0.99 |

The free-cluster results are shown in table 3. Almost independent of cluster size, the O atom is located in the first substrate layer and the frequency of the vertical vibrational motion is calculated to be about 400 $cm^{-1}$. The large Mulliken charge of −0.8 au and the small value of the induced dipole moments indicate a lateral charge transfer to the adsorbate as in the case of H adsorption. The largest cluster $Li_{38}$ is included to demonstrate that the close similarity of the results of $Li_{26}$ and $Li_{30}$ is deceptive: cluster convergency has not yet been reached. The results are in qualitative agreement with those of a Hartree–Fock study employing only double-layered clusters of up to nine substrate atoms [44]. There, an average adsorption height of −0.02 Å and a frequency of 420 $cm^{-1}$ for the vibration perpendicular to the surface were found. A Mulliken charge of −1.5 au for O led to the characterization of the adsorptive bond as very ionic, roughly corresponding to $(Li_n)^{2+}O^{2-}$ [44]. Our results indicate a considerably less ionic bond, in line with a recent comparative study of Hartree–Fock and LDA chemisorption cluster models [45].

While for H adsorption embedded-cluster results were already stabilized for $Li_{18}$, the inclusion of the complete second-nearest-neighbour shell of the adsorption-site atoms is necessary for O adsorption to achieve this 'convergence'. This is clearly seen in the changes

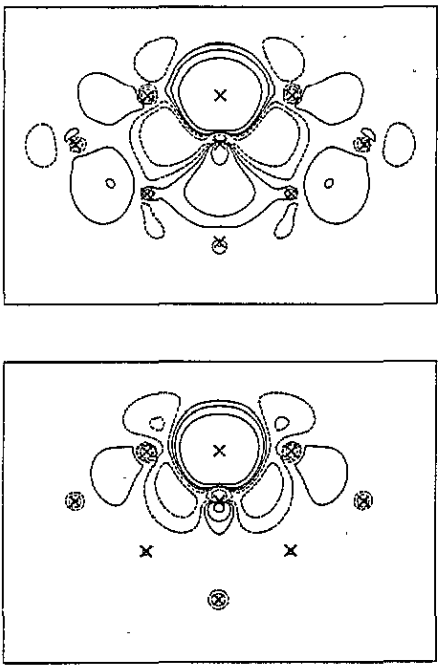

**Figure 3.** The adsorption-induced change of the electronic density $\Delta\rho = \rho(Li_{30}O) - \rho(Li_{30}) - \rho(O)$ for O adsorption at the fourfold site of Li(001): upper panel, free cluster; lower panel, embedded cluster. Contour lines are drawn for $\pm 0.00032$, $\pm 0.001$, $\pm 0.0032$ au; continuous and dashed lines correspond to positive and negative values, respectively. Crosses indicate the positions of the atoms.

of the adsorption height and of the induced dipole moment with increasing cluster size. The two largest clusters yield a geometry and a vibrational frequency in agreement with the free-cluster models. Embedding lowers the binding energy by more than 1 eV for all clusters. The induced dipole moment is found to be small, as in the case of free clusters, but negative; the charge transfer to the adsorbate is slightly enhanced.

**Table 4.** O at the fourfold site of Li(100): changes of Mulliken populations due to adsorption for free- and embedded-cluster models. See figure 1 for the designation of Li atoms.

| | Li | | | | | | | | |
|---|---|---|---|---|---|---|---|---|---|
| Cluster | $II_1$ | $I_1$ | $II_2$ | $III_1$ | $IV_1$ | $II_3$ | $I_2$ | $IV_2$ | O |
| Free | | | | | | | | | |
| $Li_{17}$ | 0.20 | 0.21 | −0.03 | −0.04 | | −0.01 | | | −0.75 |
| $Li_{18}$ | 0.11 | 0.22 | −0.01 | −0.02 | −0.02 | −0.02 | | | −0.76 |
| $Li_{26}$ | 0.17 | 0.25 | 0.02 | −0.06 | −0.01 | 0.00 | −0.03 | | −0.76 |
| $Li_{30}$ | 0.19 | 0.25 | 0.02 | −0.07 | 0.01 | −0.02 | −0.02 | 0.00 | −0.77 |
| Embedded | | | | | | | | | |
| $Li_{17}$ | 0.09 | 0.15 | 0.05 | 0.00 | | 0.03 | | | −0.96 |
| $Li_{18}$ | 0.03 | 0.18 | 0.05 | 0.01 | 0.00 | 0.02 | | | −1.00 |
| $Li_{26}$ | −0.03 | 0.20 | 0.04 | −0.01 | 0.00 | 0.00 | −0.01 | | −0.88 |
| $Li_{30}$ | 0.06 | 0.23 | 0.02 | 0.00 | −0.01 | 0.00 | −0.01 | 0.00 | −0.99 |

A strong effect of embedding is expected for the adsorption-induced charge rearrangement due to the introduction of boundary conditions. This is clearly seen in the changes of Mulliken populations summarized in table 4. Free clusters exhibit strong changes for the atoms $II_1$ and $I_1$ forming the adsorption site, the third-layer atom $III_1$ is also slightly affected. For embedded clusters the lateral charge transfer to the adsorbate is confirmed irrespective of the cluster size. Only the first-layer site atoms $I_1$ show a considerable loss of electronic charge. The vanishing change of populations for the border atoms $I_2$, $II_3$ and $IV_2$ indicates that $Li_{26}$ and $Li_{30}$ are large enough as chemisorption clusters, fulfilling the MLEC assumptions. The differences between the populations for free and embedded clusters may be explained by polarization differences of the models. These differences are more clearly demonstrated by plots of the adsorption-induced changes of density (see figure 3 for the example of $Li_{30}$). For both free and embedded clusters, a charge depletion around the O adsorbate is found. The assumption of predominantly lateral charge transfer, more obvious in the case of the embedded cluster, is supported by the observation that the top-layer site atoms $I_1$ are charged slightly negatively, while the nearest-neighbour atom of the adsorbate $II_1$ is mainly polarized. The density plots render the difference in the cluster polarization even more visible than the population analysis. While O adsorption affects the free cluster everywhere, embedding leads to a confinement of the adsorption-induced polarization to the immediate surroundings of the adsorption site. Although the perturbation due to O adsorption is considerably stronger than that due to H adsorption, again the third- and fourth-layer border atoms are found to be only slightly affected.

## 4. Summary

A modified version of the MLEC approach for cluster embedding, implemented in the framework of density-functional theory, has been presented and applied to atomic adsorption on the Li(001) surface. Pertinent new features include the use of a periodic voluminous metal substrate, the removal of the pole in the MLEC matrix that prevents the embedding of metal clusters, the substantial improvement of the SCF stability due to the self-consistent determination of the local Fermi energy and the optimization of the adsorption geometry for each cluster considered. Free- and embedded-cluster models of different size have been used in comparison to characterize the effects of embedding. For unperturbed clusters as well as for H adsorption at an on-top site it was demonstrated that the positive surface polarization found for Li(001) is successfully modelled by embedded clusters. In the case of H and O adsorption at the fourfold site it was shown that embedding leads to a reduction of the high polarizability of free-cluster models that originates in their unphysical boundary conditions. The general trend to lower adsorption energies due to embedding, already observed for H adsorption on an Li monolayer, is confirmed by nearly all examples studied in the present work. A 'moderately large' cluster, as required for a reliable application of the MLEC scheme, has to include at least the second-nearest neighbours of the substrate atoms forming the adsorption site. This size is found to be sufficient even for a strong perturbation such as O adsorption at an open surface site. In the case of insufficient cluster size the embedding leads to an overestimation of the adsorbate–substrate bond length and correspondingly to low binding energies. These observations render previous results on $H_2$ adsorption at Li(001) [27], which were achieved by using very small clusters, questionable.

**Acknowledgments**

We are indebted to B Reichert for advising us in the use of the 2D STO LDA code. We thank U Birkenheuer for many valuable discussions and for assistance with the interfacing of the STO LDA code and the LCGTO LDA cluster program. This work has been supported by the Deutsche Forschungsgemeinschaft via SFB 338 and by the Fonds der Chemischen Industrie.

## References

[1] Siegbahn P E M and Wahlgren U 1991 *Metal-Surface Reaction Energetics. Theory and Application to Heterogeneous Catalysis, Chemisorption, and Surface Diffusion* ed E Shustorovich (New York: VCH) p 1
[2] Ruette F, Sierraalta A and Hernandez A J 1992 *Quantum Chemistry Approaches to Chemisorption and Heterogeneous Catalysis* ed F Ruette (Dordrecht: Kluwer) p 256
[3] Pacchioni G, Bagus P S and Parmigiani F (ed) 1992 *Cluster Models for Surface and Bulk Phenomena (NATO ASI Series 283)* (New York: Plenum)
[4] Görling A, Ackermann L, Lauber J, Knappe P and Rösch N 1993 *Surf. Sci.* **286** 26
[5] Dunlap B I and Rösch N 1990 *Adv. Quantum Chem.* **21** 317
[6] Panas I, Schüle J, Siegbahn P and Wahlgren U 1988 *Chem. Phys. Lett.* **149** 265
[7] Rösch N, Sandl P, Görling A and Knappe P 1988 *Int. J. Quantum Chem.* S **22** 275
[8] Whitten J L and Pakkanen T A 1980 *Phys. Rev.* B **21** 4357
[9] Whitten J L 1993 *Chem. Phys.* **177** 387
[10] Colbourn E A 1992 *Surf. Sci. Rep.* **15** 281
[11] Williams A R, Feibelman P J and Lang N D 1982 *Phys. Rev.* B **26** 5433
[12] Feibelman P J 1985 *Phys. Rev. Lett.* **54** 2627
[13] Feibelman P J 1989 *Phys. Rev.* B **39** 4866
[14] Baraff G A and Schlüter M 1986 *J. Phys. C: Solid State Phys.* **19** 4383
[15] Pollmann J, Krüger P, Mazur A and Wolfgarten G 1985 *Surf. Sci.* **152** 977
[16] Scheffler M, Droste C, Fleszar A, Maca F, Wachutka G and Barzel G 1991 *Physica* B **172** 143
[17] Kirtman B and de Melo C 1981 *J. Chem. Phys.* **75** 4592
[18] Matos M, Kirtman B and de Melo C 1988 *J. Chem. Phys.* **88** 1019
[19] Pisani C 1978 *Phys. Rev.* B **17** 3143
[20] Pisani C, Dovesi R and Carosso P 1979 *Phys. Rev.* B **20** 5345
[21] Pisani C, Dovesi R and Ugliengo P 1983 *Phys. Status Solidi* b **116** 249
[22] Pisani C, Nada R and Kantorovich L 1990 *J. Chem. Phys.* **92** 7448
[23] Pisani C, Dovesi R, Nada R and Tamiro S 1989 *Surf. Sci.* **216** 489
[24] Pisani C, Orlando R and Cora F 1992 *J. Chem. Phys.* **97** 4195
[25] Pisani C, Dovesi R and Ugliengo P 1983 *Phys. Status Solidi* b **116** 547
[26] Ravenek W and Geurts F M M 1986 *J. Chem. Phys.* **84** 1613
[27] Fukunishi Y and Nakatsuji H 1992 *J. Chem. Phys.* **97** 6535
[28] Parr R G and Yang W 1989 *Density Functional Theory of Atoms and Molecules* (Oxford: Oxford University Press)
[29] Eschrig H 1988 *Optimized LCAO Method and the Electronic Structure of Extended Systems* (Berlin: Akademie)
[30] Reichert B and Jung C 1990 *Phys. Status Solidi* b **158** K119
[31] Krüger S, Birkenheuer U and Rösch N *J. Electron. Spectrosc. Relat. Phenon.* at press
[32] Carlson B C and Keller J M 1957 *Phys. Rev.* **105** 102
[33] Vosko S H, Wilk L and Nusair M 1980 *Can. J. Phys.* **58** 1200
[34] Monkhorst H J and Pack J D 1976 *Phys. Rev.* B **13** 5188
[35] Dunning T H and Hay P J *Modern Theoretical Chemistry* vol 3, ed H F Schaeffer III (New York: Plenum) p 1
[36] Van Duijneveldt F B 1971 *IBM Research Report* RJ 945
[37] Wyckoff R W G 1963 *Crystal Structures* 2nd edn (New York: Interscience)
[38] Krüger S and Rösch N 1993 *Chem. Phys. Lett.* **216** 435
[39] Birkenheuer U, Boettger J C and Rösch N 1993 unpublished results
[40] Gatti C, Fantucci P and Pacchioni G 1987 *Theor. Chim. Acta* **72** 432
[41] Pettersson L G M and Faxen T 1993 *Theor. Chim. Acta* **85** 345

[42] Beckmann H-O and Koutecký J 1982 *Surf. Sci.* **120** 127
[43] Ray A K and Hira A S 1988 *Phys. Rev.* B **37** 9943
[44] Hermann K and Bagus P S 1978 *Phys. Rev.* B **17** 4082
[45] Pacchioni G, Neyman K M and Rösch N *J. Electron. Spectrosc. Relat. Phenom.* at press